Heliyon 10 (2024) e25553

Contents lists available at ScienceDirect

Heliyon

journal homepage: www.cell.com/heliyon

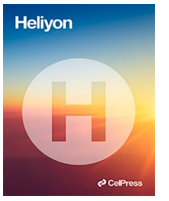

Research article

Novel BRET combination for detection of rapamycin-induced protein dimerization using luciferase from fungus *Neonothopanus nambi*

Aaiyas Mujawar [a,b], Shalini Dimri [a,b], Ksenia A. Palkina [c,d], Nadezhda M. Markina [c,d], Karen S. Sarkisyan [c,d,e], Anastasia V. Balakireva [c,d], Ilia V. Yampolsky [c,d,**], Abhijit De [a,b,*]

[a] *Advanced Center for Treatment Research and Education in Cancer (ACTREC), Sector-22, Kharghar, Navi Mumbai 410210, India*
[b] *Life Science, Homi Bhabha National Institute, Mumbai, India*
[c] *Planta LLC, Bolshoi Boulevard, 42 Str 1, Moscow, Russia*
[d] *Shemyakin-Ovchinnikov Institute of Bioorganic Chemistry of the Russian Academy of Sciences, Miklukho-Maklaya, 16/10, Moscow, Russia*
[e] *Synthetic Biology Group, MRC London Institute of Medical Sciences, London W12 0NN, UK*

ARTICLE INFO

Keywords:
Bioluminescence resonance energy transfer
Luciferase
Cancer
Cell signaling
Rapamycin
Fungal BRET
mTOR signalling

ABSTRACT

Bioluminescence resonance energy transfer (BRET) is one of the most promising approaches used for noninvasive imaging of protein-protein interactions *in vivo*. Recently, our team has discovered a genetically encodable bioluminescent system from the fungus *Neonothopanus nambi* and identified a novel luciferase that represents an imaging tool orthogonal to other luciferin-luciferase systems. We demonstrated the possibility of using the fungal luciferase as a new BRET donor by creating fused pairs with acceptor red fluorescent proteins, of which tdTomato provided the highest BRET efficiency. Using this new BRET system, we also designed a mTOR pathway specific rapamycin biosensor by integrating the FRB and FKBP12 protein dimerization system. We demonstrated the specificity and efficacy of the new fungal luciferase-based BRET combination for application in mammalian cell culture that will provide the unique opportunity to perform multiplexed BRET assessment in the future.

1. Introduction

Protein-protein interactions (PPIs) form the basis of cellular functions and biological processes in living organisms. When studying PPI it is important to preserve the native protein structure and subcellular localization. This can be achieved using noninvasive bioimaging methods that follow Förster resonance energy transfer principles such as fluorescence resonance energy transfer (FRET) [1, 2] and bioluminescence resonance energy transfer (BRET) [3]. FRET and BRET require two or more photoactive molecules — a donor

* Corresponding author. Molecular Functional Imaging Lab, Advanced Centre for Treatment, Research and Education in Cancer, Navi Mumbai, India.
** Corresponding author. Institute of Bioorganic Chemistry (IBCh), Russian Academy of Sciences, Moscow, Russia.
E-mail addresses: aaiyasmujawar@gmail.com (A. Mujawar), yashree.dimri@gmail.com (S. Dimri), kpalkina93@gmail.com (K.A. Palkina), markina.nadya@gmail.com (N.M. Markina), karen@planta.bio (K.S. Sarkisyan), balakireva.anastacia@gmail.com (A.V. Balakireva), ivyamp@gmail.com (I.V. Yampolsky), ade@actrec.gov.in (A. De).

https://doi.org/10.1016/j.heliyon.2024.e25553
Received 8 July 2023; Received in revised form 18 January 2024; Accepted 29 January 2024
Available online 8 February 2024

and an acceptor situated at a specific orientation and interacting with each other at a very short distance (<10 nm). Resonance energy transfer from the excited donor to the acceptor molecule, which emits light at its characteristic wavelength [4,5]. Approaches based on BRET are favored over FRET ones since they do not require the external light for excitation of the donor molecule, and the luciferin-luciferase reaction is the sole source of energy transfer to the fluorophore. Luciferases possessing different spectral characteristics compared with well-established ones open up the scope of BRET applications [6]. The BRET assay can be used to study protein-protein interaction when both the interactors are known. However, it requires successful generation of the fusion proteins which may be difficult to generate sometimes, particularly for proteins with higher molecular weight or with complex folding properties and thereby limiting the application of this assay. BRET has been used to study a wide variety of PPIs and/or ligand mediated PPIs [7]. Fluorescent ligands have been used to study ligand interaction based activation and PPI of G-protein coupled receptors using BRET [8]. Novel bioluminescent donors will also promote multicolor BRET imaging for the monitoring of multiplexed events simultaneously inside the cell [9–11].

Recently, we have described the bioluminescent system from the fungus *Neonothopanus nambi* and identified the intermediates of the luciferin biosynthetic pathway [12]. This biochemical cascade was successfully applied for genetically encoding the bioluminescent phenotype in eukaryotes [13]. Fungal luciferase as well as its substrate, 3-hydroxyhispidin, differs from other known and commonly used luciferin-luciferase systems. This luciferase-luciferin pair also represents distinctive emission maxima (Em_{Max}) of is 525 nm. However, whether or not this enzyme is suitable for use as a BRET donor and can be utilized for characterizing PPIs remains unknown. The addition of nnLuz based BRET sensor will help in multiplexing orthogonal BRET sensors to analyze the complex interactomics of the cells in realtime as nnLuz and 3-hydroxyhispidin show no cross reactivity with known luciferase-substrate pairs. It also provides option of a BRET sensor in 520–540 nm range with glow kinetics compared to RLuc based BRET sensors.

A macrolide antibiotic rapamycin forms a complex with human FK506 binding protein 12 (FKBP12), which subsequently directly heterodimerizes with the FKBP12-rapamycin binding domain (FRB) in live-cultured mammalian cells [14–16]. The rapamycin-FKBP12 complex interferes with the target of rapamycin complex 1 (TORC1) function by binding to its FRB domain [17]. mTOR kinase is essential for cell growth and proliferation, cell motility, survival, synthesis of proteins, autophagy, and transcription in both healthy and cancer cells [17]. mTOR inhibitors prevent transplant rejection [18] and play an important role in anticancer [19] and anti-aging therapies [20]. The development of sensors specific for FKBP12-FRB interaction is required for screening of mTOR inhibitors (e.g. rapamycin analogs). We have performed a thorough donor-acceptor match pairing of the fungal luciferase with two different fluorescent proteins (FPs) and report for the first time the development of new BRET combinations using the fungal luciferase from *N. nambi* (nnLuz). Further, we have tested the specificity and efficacy of the new BRET system by developing a FKBP12-FRB biosensor, which responds to rapamycin addition in nanomolar range.

2. Results

2.1. Selection of an optimal acceptor for fungal luciferase-based BRET combination in mammalian cells

The primary stage in the engineering of a BRET sensor is the search for an optimal donor-acceptor protein pair. Since nnLuz has a broad emission range with λ_{em} at 525 nm and extended shoulder up to 625 nm, we primarily chose FPs, which maximally absorb photon energy (Ex_{Max}) in the 550–580 nm range: tdTomato, and mRuby2 (Supplementary Table 1), and engineered fusion proteins consisting of nnLuz and the selected FPs. All BRET ratio were represented in mBRET units (mBU) using Eq. (1) [7].

We also aimed to determine the optimal molecular distance between nnLuz and tdTomato or mRuby2, which may affect the energy transfer. To identify linker length and sequence, which would lead to the highest BRET efficiency, we tested a number of different

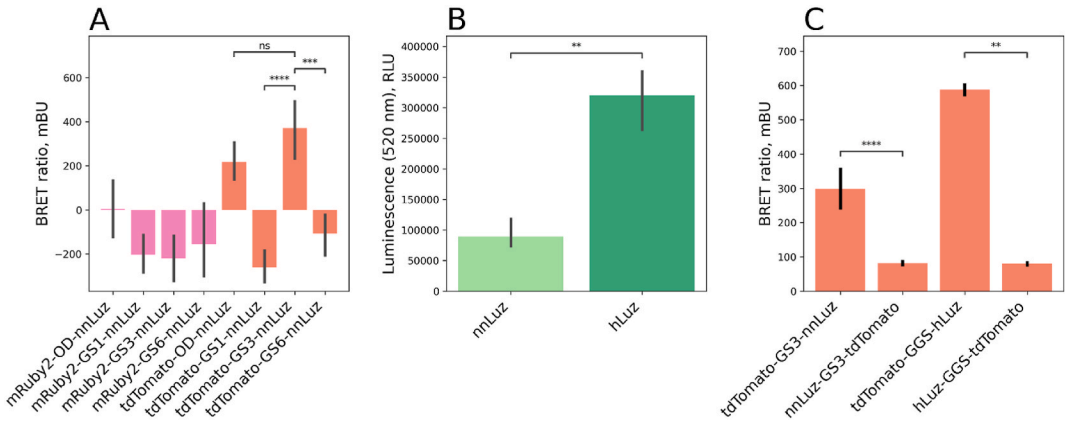

Fig. 1. Optimizing the BRET pair structure. (A) Determination of the optimal FP acceptor and linker length. (B) Optimizing the luciferase gene expression after codon optimization for human (hLuz) using HT1080 human cell line. (C) Selecting the optimal mutual orientation. GS — glycine-serine rich linker, $GS_n = (GGGGS)_n$, GGS = $(GGS)_4$, nnLuz — wild-type coding sequence of *Neonothopanus nambi* luciferase, hLuz — human codon-optimized coding sequence of *N. nambi* luciferase. Each bar represents mean value ± SEM, *p < 0.05, **p < 0.01, ***p < 0.001, ****p < 0.0001.

linkers as shown in Supplementary Table 2. We have tested primarily glycine-serine rich linkers (i.e. GS1, GS3, and GS6) consisting of GGGGS motif repeated one, three, or six times, thus providing linkers with 5 a.a., 15 a.a. and 30 a.a. length, respectively. We have also attempted the so-called OD-linker, which was successfully used for the engineering of BRET pairs based on *Renilla* luciferase [21]. We have chosen to place FPs at the N-terminus of nnLuz for the first round of BRET pair selection. Fusion protein genes were put under the control of cytomegalovirus (CMV) promoter and simian virus 40 (SV40) polyadenylation signal. We tested resulting fusion constructs via transient transfection of human fibrosarcoma cell line HT1080. The acceptor tdTomato linked to nnLuz at N-terminus by either GS3- or OD-linker has shown higher BRET efficiency (milliBRET unit, or mBU) compared to all mRuby2 as acceptor protein. The BRET efficiency of tdTomato-containing fusions linked to nnLuz by GS3-or OD-linker were also found superior than constructs prepared using GS1- or GS6-linker (Fig. 1A).

Next, considering the primary use of BRET pair in human cells, a human codon-optimized nnLuz (viz. hLuz) gene was generated by

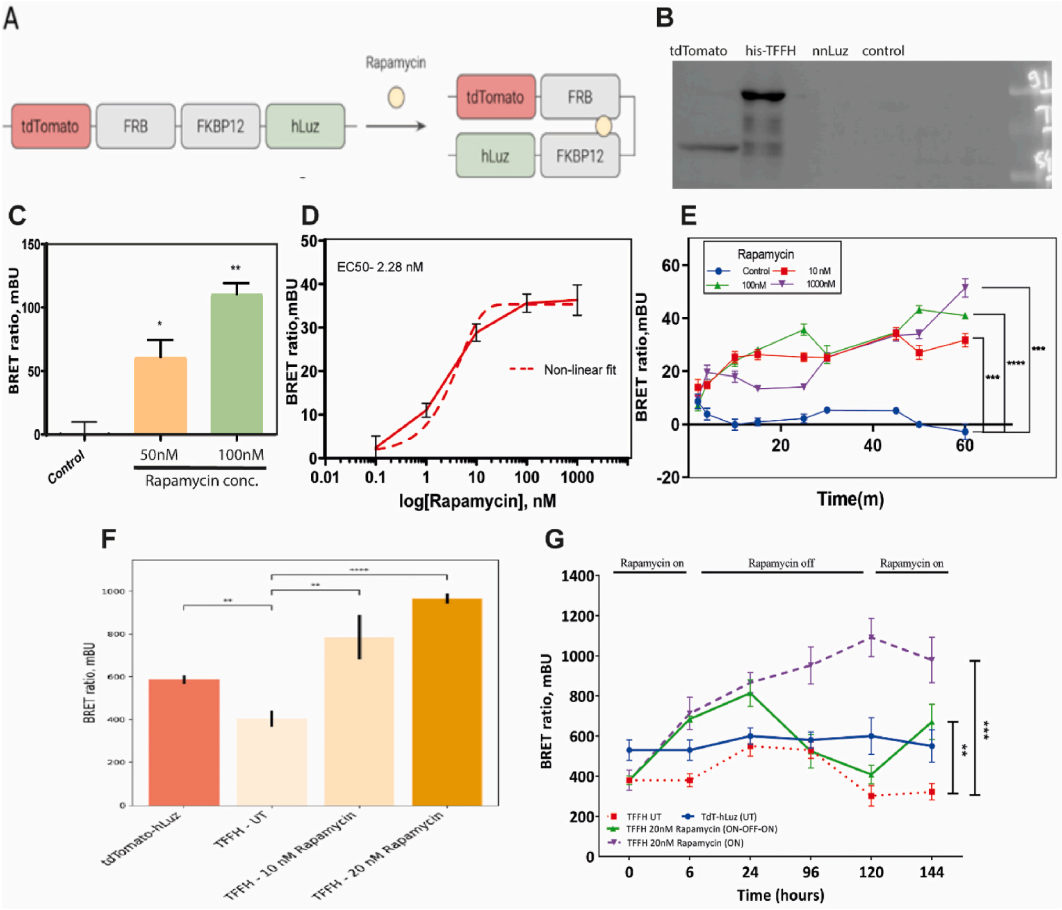

Fig. 2. hLuz-based BRET sensor enabled effective detection of the rapamycin-induced FRB-FKBP12 heterodimer formation. (A) The schematic representation of the working principle of the TFFH sensor. (B) Immunoblot showing intact His-tagged TFFH BRET fusion expression probed with tdTomato mAb. The tdTomato, nnLuz purified extracts and untransformed *E. coli* BL21 lysate were used as control. (C) Bar graph showing the BRET ratio measured from His-tag purified TFFH fusion protein treated with 50 nM and 100 nM of rapamycin along with untreated control. (D) The graph showing BRET ratio obtained from HT1080 cells stably expressing TFFH sensor construct treated with Rapamycin (0.1–1000 nM) for 1 h (The dotted line indicates the non-linear regression fit). (E) Graph showing time kinetics of BRET signal of HT1080 cells stably expressing the TFFH sensor treated with rapamycin (10, 100 and, 1000 nM) for 1 h and BRET ratio was measured for time 2, 5, 10, 15, 20, 30, 45 and 60 min after rapamycin addition. (F) The graph showing BRET ratio obtained from HT1080 cells transfected with TFFH in the absence of rapamycin (untreated) and rapamycin-treated condition (10, 20 nM); tdTomato-GGS-hLuz fusion protein was used as a positive control. (G) HT1080 cells overexpressing the TFFH sensor were tested for the switch on/off function in the presence or absence of 20 nM rapamycin. In the graph, BRET ratio was measured at multiple time points (0, 6, 24, 96, 120, 144 h); the experimental sample (green solid line) was first incubated with 20 nM rapamycin for 0–6 h; then drug was withdrawn and cells were incubated in plain media till imaged at 120 h; cells were treated again with 20 nM rapamycin at 120–144 h, as indicated above. TFFH-expressing cells not treated with rapamycin were kept as negative control (blue solid line) and treated with 20 nM rapamycin for the entire duration of 0–144 h as a positive control (purple dashed line). The tdTomato-hLuz overexpressing cells were kept as BRET standard control (red dotted line). TFFH — tdTomato-FRB-FKBP12-hLuz. Each bar or point represents mean value ± SEM, *$p < 0.05$, **$p < 0.01$, ***$p < 0.001$. ****$p < 0.0001$ (The full, non-adjusted immunoblot image are shown in Supplement file-Fig. S2B). (For interpretation of the references to color in this figure legend, the reader is referred to the Web version of this article.)

using GeneOptimizer tool [22]. Compared to the native nnLuz, the equivalent amount of hLuz plasmid transfected in HT1080 cell line yielded about 4-fold higher photon output (Fig. 1B). It's worth noting here that though the photonic output changed significantly when human codon optimized hLuz was expressed as compared to nnLuz (Supplementary Fig. 1); however, no apparent change in photon output or BRET efficiency realized when the donor was fused with various acceptor proteins. Further, by replacing the GS3 (15 amino acid) with GGS (12 amino acid) linker, impact of molecular length on the BRET efficiency of the pair was studied (Supplementary Table 2). The 12-mer GGS peptide linker, which was extensively tested in our laboratory before [23], showed a clear improvement in efficiency for the tdTomato-hLuz BRET combination (Fig. 1C). Thereafter, we generated BRET pairs for the hLuz donor with tdTomato in all possible orientations (i.e. either N-terminus or C-terminus fusion), while maintaining the optimized linker length as 12 amino acid residues. Acceptor (tdTomato) and donor specific spectral photon output was measured by using 520 ± 20 nm donor and 580 ± 20 nm acceptor bandpass filters and the BRET ratio was calculated as per Eq. (1) shown in methods section. The highest BRET efficiency ($p < 0.005$) was obtained from the tdTomato-GGS-hLuz fusion (Fig. 1C).

2.2. The tdTomato-hLuz BRET biosensor designed for studying FRB and FKBP12 interaction showed efficient energy transfer in live-cell conditions

We chose tdTomato-hLuz BRET pair for the development of a BRET biosensor for detection of a rapamycin-mediated interaction between human FKBP12 and FRB protein domains *in vivo* live cell condition [14]. The FRB and FKBP12 coding sequences were subcloned in frame by replacing parts of the 12 a.a. linker in the tdTomato-GGS-hLuz BRET plasmid vector. The resulting construct coded for tdTomato-FRB-FKBP12-hLuz (TFFH). Upon treatment with rapamycin FRB and FKBP12 heterodimerize; this interaction can be characterized by the efficiency of energy transfer between hLuz and tdTomato in a rapamycin concentration-dependent manner (Fig. 2A). Comparison to the similar already reported rapamycin biosensor $TurboFP_{635}$-FRB-FKBP12-NanoLuc (TFFN), the energy transfer efficiency was found superior (Supplementary Note 1 and Supplementary Fig. 2).

First, the TFFH fusion protein expression was validated by performing immunoblotting using tdTomato mAb for probing in both purified bacterial extract as well as in mammalian cell expression. The result showed presence of intact fusion with an elevated molecular weight as compared to the tdTomato protein that was used as positive control (Fig. 2B and Supplementary Fig. 3). We further perform purification of 6xHis-TFFH (his-TFFH) sensor using inducible bacterial expression system (Supplementary note 3). As compared to untreated protein, rapamycin treated his-TFFH protein showed significant increase in BRET ratio, i.e. for 50 nM ($p = 0.037$) or 100 nM ($p = 0.007$) (Fig. 2C). Further, results also showed an exponential increase in BRET signal in HT1080 cell line stably expressing TFFH sensor after treatment 1 h of 0.1–1000 nM of rapamycin treatment (Fig. 2D). Over here, we observed an exponential increment in BRET signal with rapamycin concentration till 10 nM. Beyond 10 nM of rapamycin treatment the BRET signal gets saturated. The EC_{50} for rapamycin was calculated to be 2.2 nM in HT1080 cell line. The time kinetics assay shows significant increase in BRET signal just after 10 min of 10 nM and 100 nM rapamycin ($p = 0.002$ and $p < 0.001$) treatment in HT1080 cell line stably expressing TFFH sensor. The steady increase in BRET signal continued till 1 h of rapamycin treatment (Fig. 2E).

We opted for a 10 nM and 20 nM dose in our further experiments as 10–100 nM dose escalation only gave a marginal gain in the BRET signal. We observed ~2-fold higher BRET signal after 6 h of 10 nM rapamycin treatment of TFFH expressing cells compared to the untreated TFFH ($p < 0.01$) or the control tdTomato-hLuz fusion ($p < 0.001$). In addition, mean mBU value registered for TFFH fusion protein after 6 h of 20 nM rapamycin treatment was even higher compared to 10 nM. This result indicates that the donor and acceptor approximated after rapamycin treatment (Fig. 2F). Together, these results confirmed that the TFFH fusion reporter is a functional biosensor and showed concentration dependent BRET increment in HT1080 cells.

To further assess the sensitivity of the TFFH sensor, we determined the kinetics of the BRET ratios fluctuation in an on/off rapamycin cycle. For this, in the experimental line, we treated the HT1080 cells expressing the TFFH sensor with 20 nM rapamycin (Fig. 2G) for 6 h, withdrew it by maintaining the cells in live culture, and then registered the kinetics for following 5 days, followed by a second pulse of rapamycin on the 6th day. Live-cell measurement of BRET showed a significant increase in BRET signal within 6 h of rapamycin treatment ($p < 0.05$). The interaction between FRB and FKBP12 that occurred upon first exposure to rapamycin has led to the increased BRET signal (6 h). It took almost 120 h for the BRET signal to drop to the basal level ($p < 0.001$) in the absence of rapamycin during the following days. The requirement of a few days for the BRET signal to reduce in the absence of rapamycin indicated no new rapamycin dependent FRB-FKBP12 heterodimers formed in the experimental line. Further, when rapamycin was added in the wells for the second time, the BRET signal elevated back ($p < 0.01$). As a positive control we used cells under continuous exposure to rapamycin. They showed a constant elevation of BRET signal for up to 5 days before achieving saturation ($p < 0.001$). The untreated control cells and cells expressing tdTomato-GGS-hLuz control BRET pair showed insignificant change in BRET signal (Fig. 2G). These results highlight that the tdTomato-hLuz BRET system can selectively reflect molecular interaction caused by rapamycin and report kinetics of the FRB-FKBP12 dimerization in real time from live cell population.

2.3. BRET sensor tdTomato-FRB-FKBP12-hLuz containing mutant FRB protein shows an inability of FRB and FKBP12 to heterodimerize

For further validation of the TFFH sensor specificity, we introduced two point mutations: A2034V and F2108L in the rapamycin-binding site of FRB domain using site-directed mutagenesis [24,25]. The two mutated TFFH sensors were expected to become insensitive to the rapamycin treatment: thus, the donor-acceptor proximity would not be achieved resulting in no gain of BRET signal. In the HT1080 cells expressing wild-type TFFH sensor BRET signal value increased by one order of magnitude upon treatment with 20 nM rapamycin ($p < 0.001$) in comparison to untreated control. In contrast, the A2034V mutant exhibited a minor but significant increase in the BRET ratio: positive value after 20 nM rapamycin treatment compared to negative value for untreated control ($p < 0.05$)

(Fig. 3A).

We have also evaluated the effect of a second point mutation, F2108L. The BRET sensor bearing this mutation failed to show any significant gain in BRET ratio, showing similar values for untreated conditions and for 20 nM rapamycin-treated conditions (non-significant difference) (Fig. 3B). These observations were closely replicated in the MCF7 breast cancer cell line (Fig. 3C and D). Taken together, these results clearly indicate that hLuz and tdTomato represent a compatible donor-acceptor pair showing PPI-specific resonance energy transfer in live-cell conditions.

3. Discussion

In the present study we explored the suitability of using the recently discovered fungal luciferase isolated from *N. nambi* as a novel BRET donor and showed its potential for detection of PPI using rapamycin-induced FRB and FKBP12 heterodimerization in human cell lines. This new fungal luciferase possesses distinct features for use as a new BRET donor due to its natural emission in the green spectrum of light (Em_{Max} = 525 nm). It also does not cross-react with other known luciferases so far reported and used for BRET combinations. Therefore, the possible development of a multiplexed BRET assay is envisioned (Fig. 4) [23,26,27].

We showed that fungal luciferase can serve as a donor for a number of acceptor red fluorescent proteins with spectral overlap (i.e. tdTomato and mRuby2), out of which the most suitable acceptor protein appeared to be tdTomato. Some of the fusion constructs showed negative BRET ratio indicating lower photon output in BRET than the donor alone. The lower photon output in BRET construct is possible as a result of fusion with the fluorescent protein.

Considering possible applications of the new BRET pairs in human cell-based screening, we also generated a BRET pair using a human codon-optimized nnLuz (hLuz) that appeared to be several folds brighter than wild-type nnLuz presumably because of the efficient expression level in human cells. We also demonstrated the use of glycine-serine rich flexible linkers that the molecular

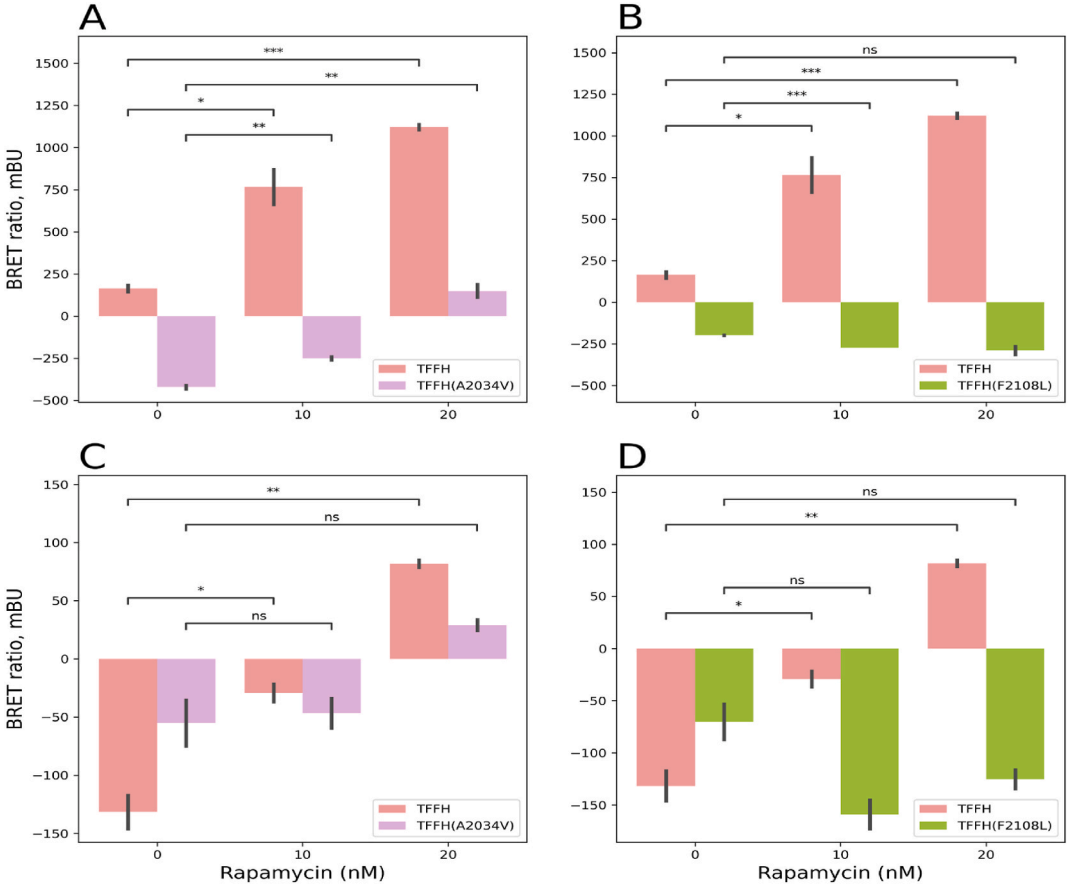

Fig. 3. Effect of FRB domain point mutations on BRET signal in HT1080 and MCF7 cell lines. (A–B) BRET signal measured for TFFH sensor construct incorporated with A2034V mutant or F2108L mutant transfected in HT1080 cell line. BRET was measured after 6 h of rapamycin treatment (10 nM and 20 nM) and compared with untreated control. (C–D) BRET signal for TFFH sensor construct incorporated with A2034V mutant or F2108L mutant transfected in MCF7 cell line. BRET was measured after 6 h of rapamycin treatment (10 nM and 20 nM) and compared with untreated control. Each bar represents mean value ± SEM, *p < 0.05, **p < 0.01, ***p < 0.001, ns — non-significant. (The full, non-adjusted immunoblot image are shown in Supplement file-Fig. S3).

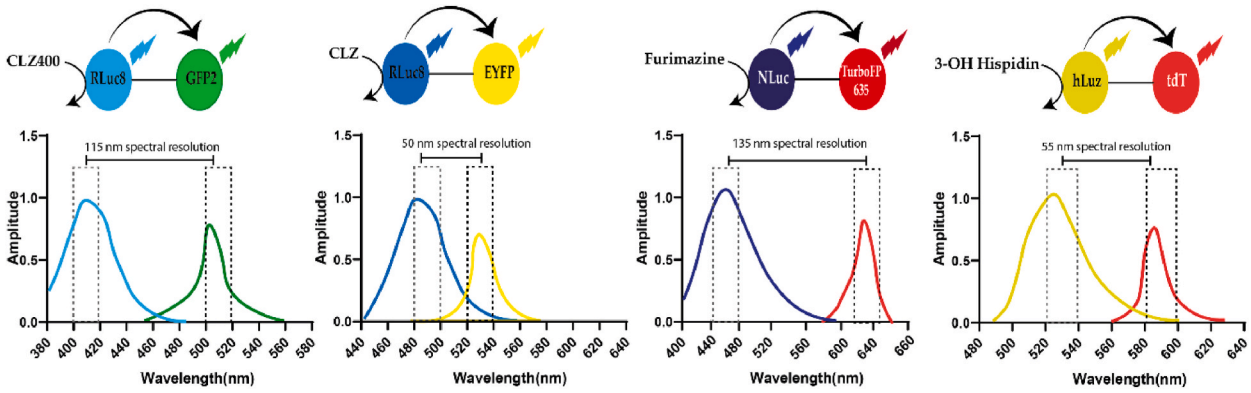

Fig. 4. Diagrammatic representation of multiplexed BRET concept indicating representative spectral characteristics of existing BRET-pairs i.e. RLuc8-GFP2, RLuc8-EYFP, NanoLuc-TurboFP635 and the current hLuz-tdTomato BRET pair that could be used together for development of multiplexed BRET assays.

distance equivalent to 12 amino acids resulted in the maximal BRET ratio as found in the case of tdTomato-hLuz pair.

Further, taking the help of a well-validated rapamycin-induced FRB-FKBP12 biological model, we have demonstrated how the tdTomato-hLuz BRET pair can be taken forward to develop a sensor for monitoring PPIs directly in live cells. In presence of rapamycin purified his-TFFH protein showed increased BRET signal indicating the sensor is sufficiently sensitive for sensing the drug action and it could be a good option for *in vitro* screening of PPi modulators in a cell-free system. The on/off kinetics of the BRET biosensor in the presence or absence of rapamycin clearly demonstrates the specificity of the system tested for detection of signal kinetics from live-cell culture and gives a clear readout of the dimerization-dependent resonance energy transfer status *in vivo*. Furthermore, using F2108L or A2034V mutants of FRB protein we also demonstrated that upon abrogation of rapamycin binding to the FRB domain no non-specific activation of BRET signal was recorded. These results clearly suggest that the developed sensor is highly specific for the mTOR pathway and may be suitably used to determine rapamycin concentration and, potentially, to screen activity of rapamycin analogs. We have thoroughly validated the developed BRET sensor for cell-based application. In future, to address complex biology problems involving multiple protein interactions requiring multiplexed BRET assay may suitably adapt this new BRET pair along with other known BRET pairs for use as *in vitro* or *in-vivo* studies.

4. Materials and methods

4.1. Plasmid cloning

All genetic constructs of nnLuz for mammalian cell transfection with potential BRET pair fluorescent protein genes were created using the standard protocol of Golden Gate MoClo technology [28]. All Golden Gate cloning reactions were performed in 1× T4 ligase buffer (ThermoFisher) containing 10U of T4 ligase, 20U of BsaI (ThermoFisher), and 100 ng of DNA of each DNA part. Golden Gate reactions were performed 25 cycles between 37 °C and 16 °C (90 s at 37 °C, 180 s at 16 °C). The final vector included CMV promoter, fungal luciferase gene, amino acid linker coding sequence, fluorescent protein gene (tdTomato, mRuby2), SV40 polyadenylation signal and kanamycin resistance gene for bacterial selection. All the clones were confirmed by Sanger sequencing (Evrogen).

The human codon-optimized gene sequence of nnLuz was determined by GeneOptimizer tool (ThermoFisher), and the hLuz gene was synthesized by GeneArt technology (ThermoFisher) [22]. Genetic constructs encoding the hLuz gene with FP genes aimed to determine a potential fluorescent acceptor for the BRET pair were prepared in a pCMV empty vector containing a suitable flexible $(GGS)_4$ linker. The hLuz gene was inserted at the N-terminus by cloning a PCR-amplified full-length hLuz sequence using NheI and AgeI restriction enzymes, while PCR-amplified FP genes (tdTomato or mRuby2) were inserted at C-terminus without stop codon using EcoRI and SalI restriction enzymes. Either hLuz or NanoLuc genes were inserted at the C-terminus of FKBP12 sequence in tdTomato-FRB-FKBP12 plasmid by cloning a PCR-amplified full-length of either hLuz or NanoLuc sequence using XbaI and BamHI restriction enzymes. The final vector included CMV promoter, fungal luciferase gene, amino acid linker coding sequence, FP gene, SV40 polyadenylation signal, and Zeocin™ resistance gene for bacterial and mammalian selection. A PCR-amplified full-length TFFH sequence was cloned in frame with 6x-histidine tag in an inducible bacterial expression vector under the T7 promoter. BamHI and HindIII restriction sites were used for cloning the cassette. All clones were confirmed by restriction digestion and Sanger sequencing. The primers used are available in the Supplementary Materials (Supplementary Table 3).

4.2. Generation of FRB mutant forms

For introducing point mutations in the FRB domain, we used PCR-based site-directed mutagenesis method. The primers for introduction of A2034V and F2108L mutations are available in the corresponding section of Supplementary Materials (Supplementary Table 3). Mutations incorporated were confirmed by Sanger sequencing.

4.3. Mammalian cell lines cultivation

HT1080 were cultured in DMEM medium (Gibco) supplemented with 10% fetal bovine serum (Sigma-Aldrich) and 1% penicillin/streptomycin/amphotericin (Invitrogen). MCF7 were cultured in RPMI medium (Gibco) supplemented with 10% fetal bovine serum (Sigma-Aldrich) and 1% penicillin/streptomycin/amphotericin (Invitrogen). All the cells were maintained at 37 °C in a 5% CO_2 humidified incubator.

4.4. Immunoblotting

Whole-cell extracts were prepared using RIPA/Bacterial lysis buffer [Tris Base (50 mM), Glycerol (1%), Triton X-100 (0.1%) (pH 8)] with a proteinase inhibitor cocktail. After incubation in ice for 30 min, lysates were sonicated and collected after centrifugation at 13000 rpm for 20 min. 40 μg of protein were resolved by SDS-PAGE, transferred onto BioTrace PVDF membrane and probed using appropriate dilutions of the primary antibodies. Immunoblot detection was done by anti-rabbit secondary antibody (Supplementary Table 5). Immunoreactive protein complexes were visualized by using the WesternBright ECL kit. Image acquisition and analysis were made on ChemiDoc imaging systems (Bio-rad).

4.5. Transfection of mammalian cells

HT1080 were seeded in 12-well plates for transfection. Constructs of nnLuz, hLuz under CMV promoter and RLuc8.6 under human thymidine kinase promoter (pHTK) were used as a transfection control. Transfection was done using Lipofectamine 2000 (ThermoFisher) according to manufacturer's instructions [29]. After 24 h of transfection, the cells were trypsinized. 1×10^4 cells per well were seeded in a black 96-well plate with a clear bottom (Costar). The 96-well plate was further incubated for 24 h followed by the addition of 50 μL of 3-hydroxyhispidin (fungal luciferase substrate 1 mg/ml solution in PBS) to each well. The bioluminescent signal acquisition was done using the IVIS Spectrum (PerkinElmer).

4.6. Expression and purification of TFFH construct (bacterial expression system)

E. coli BL21 DE3 pLyss strain was used for expression and purification of TFFH fusion protein after induction with 0.4 mM IPTG for 16 h. The induced cell pellet was lysed using bacterial lysis buffer as described in immunoblotting method section. Then this lysate was passed through a column containing Ni-NTA beads (Qiagen) as per manufacturer's protocol. The purified his-TFFH protein was used to carry out validation experiments.

4.7. BRET assay

HT1080 were seeded in 12-well plates for transfection, at 70–80% confluency cells were transfected with fusion constructs of nnLuz or hLuz with different fluorescent proteins, sensors TFFH, TuFFN, TFFH(F2108L), TFFH(A2034), or NanoLuc-containing constructs using Lipofectamine 2000 (ThermoFisher). After 24 h of transfection cells were trypsinized. 4×10^4 cells per well were seeded in a black 96-well plate with a clear bottom. The 96-well plate was further incubated for 24 h and subsequently used to determine the suitable BRET partner for nnLuz and hLuz by adding 50 μL of 3-hydroxyhispidin (1 mg/ml solution) in PBS to each well. Image acquisition was done in IVIS Spectrum at donor channel (520 ± 20 nm) and acceptor channel (580 ± 20 nm for tdTomato, 600 ± 20 nm for mRuby2) with an integration time of 60 s per filter.

HT1080 and MCF7 cells were transfected with TFFH, TuFFN, TFFH(F2108L), TFFH(A2034V) and donor only constructs of hLuz and NanoLuc and were seeded in black 96-well plate as described earlier. Then the cells were treated with rapamycin (Sigma-Aldrich) in concentration 10 nM or 20 nM for 6 h. After rapamycin treatment for the tdTomato-FRB-FKBP12-hLuz BRET sensor and its mutants 50 μL of 3-hydroxyhispidin (1 mg/ml solution) in PBS was added to each well. Acquisition was done in IVIS Spectrum at donor channel (520 ± 20 nm) and acceptor channel (580 ± 20 nm) with an integration time of 60 s per filter. For $TurboFP_{635}$-FRB-FKBP12-NanoLuc sensor 50 μL furimazine (Promega) (1:1000 diluted in DMEM from main stock) was added to each well and acquisition was performed in IVIS spectrum at donor channel (500 ± 20 nm) and acceptor channel (640 ± 20 nm) with an integration time of 1 s per filter.

For *in vitro* BRET assay Ni-NTA column purified proteins from bacterial expression system, 50 μL of 30 μM of the his-TFFH fusion protein was added in a black clear bottom 96-well plate. Rapamycin (Sigma-Aldrich) small molecule drug was added at a concentration of 50 nM or 100 nM and incubated for 10 min. Image acquisition was done after adding 50 μL of 3-hydroxyhispidin (1 mg/ml solution) in PBS to each well as described earlier. BRET ratio was calculated using following Eq. (1) [7]:

$$\mathrm{BRET} = \frac{\mathrm{BL_{emission}(Acceptor)} - C_f \times \mathrm{BL_{emission}(Donor)}}{\mathrm{BL_{emission}(Donor)}}$$
$$C_f = \frac{\mathrm{BL_{emission}(Acceptor)_{donor-only}}}{\mathrm{BL_{emission}(Donor)_{donor-only}}} \quad (1)$$

Equation 1 – Equation for calculation of BRET ratio in milliBRET units (mBU)
BL emission (Acceptor) – Bioluminescence signal of BRET sensor construct or Donor–Acceptor fusion construct at acceptor channel.

BL emission (Donor) - Bioluminescence signal of BRET sensor construct or Donor–Acceptor fusion construct at donor channel.
C_f – Correction factor
BL emission (Donor) donor only-Bioluminescence signal of Donor only construct at donor channel.
BL emission (Acceptor) donor only-Bioluminescence signal of Donor only construct at acceptor channel.

4.8. BRET time kinetics assay

Long time duration assay-HT1080 cells were seeded in 12-wel plate. At the confluency of 70–80%, transfection with fusion constructs - TFFH, tdTomato-hLuz and hLuz was done using Lipofectamine 2000 reagent in separate wells. 24 h post transfection, cells were trypsinized and re-seeded at the density of 4×10^4 cells per well in 96 black-well plate with clear bottom. For TFFH cells, 3 treatment groups were created – created – a) untreated, b) 20 nM Rapamycin On (in order to maintain 20 nM Rapamycin concentration, after every 24 h media was replaced with 20 nM Rapamycin containing media), and c) 20 nM Rapamycin On-Off (20 nM Rapamycin treatment was given just for initial 6 h and after which readings was acquired at 24 h and 96 h in medium without Rapamycin. While at 120 h, 20 nM Rapamycin was added again). For all samples, readings were taken at 6 h, 24 h, 96 h, 120 h and 144 h by addition of 50 μl of 3-hydroxyhispidin (1 mg/ml solution) substrate in PBS. The acquisition was done by IVIS Spectrum at donor channel (520 ± 20 nm) and acceptor channel (580 ± 20 nm for tdTomato) with an integration time of 60 s per filter.

Short time duration assay-$2x10^4$ HT1080 cells stably expressing TFFH sensor or hLuz were seeded in 96 black well plate. Rapamycin at different concentration (0, 10,100 and 1000 nM) was added to each well followed by 50 μl of 3-hydroxyhispidin (1 mg/ml) substrate addition. Immediately after rapamycin addition IVIS image acquisition was done at donor channel (520 ± 20 nm) and acceptor channel (580 ± 20 nm for tdTomato) with an integration time of 40 s per filter. The change in luciferase activity was minimum throughout the experiment.

4.9. Statistical analysis

For all data analysis Student *t*-test (unpaired and two-sided) was employed and done by Microsoft Excel. p-value<0.05 was considered statistically significant. For each experiment at least two biological replicates and three technical replicates were performed, except the experiment with long duration rapamycin on/off switch that was performed once in three technical replicates.

Data availability statement

The data presented in this study has not be uploaded in any public database but will be made available on request from the corresponding author.

CRediT authorship contribution statement

Aaiyas Mujawar: Writing – review & editing, Writing – original draft, Validation, Methodology, Investigation, Formal analysis. **Shalini Dimri:** Writing – review & editing, Writing – original draft, Validation, Methodology, Investigation. **Ksenia A. Palkina:** Writing – review & editing, Writing – original draft, Methodology, Investigation. **Nadezhda M. Markina:** Writing – review & editing, Writing – original draft, Methodology, Investigation. **Karen S. Sarkisyan:** Writing – review & editing, Writing – original draft. **Anastasia V. Balakireva:** Writing – review & editing, Writing – original draft. **Ilia V. Yampolsky:** Writing – review & editing, Visualization, Supervision, Resources, Project administration, Funding acquisition, Conceptualization. **Abhijit De:** Writing – review & editing, Writing – original draft, Visualization, Supervision, Resources, Project administration, Funding acquisition, Data curation, Conceptualization.

Declaration of competing interest

The authors declare that they have no known competing financial interests or personal relationships that could have appeared to influence the work reported in this paper.

Acknowledgments

The reported study was funded to AD and IVY as Indo-Russia bilateral projects (ref. DST/INT/RUS/RSF/P-42/2021(G); DBT/IC-2/Indo-Russia/2017–19/01 and RSF project number 22-44-02024, https://rscf.ru/project/22-44-02024/.

Appendix A. Supplementary data

Supplementary data to this article can be found online at https://doi.org/10.1016/j.heliyon.2024.e25553.

References

[1] T.W. Gadella, T.M. Jovin, Oligomerization of epidermal growth factor receptors on A431 cells studied by time-resolved fluorescence imaging microscopy. A stereochemical model for tyrosine kinase receptor activation, J. Cell Biol. 129 (1995) 1543–1558, https://doi.org/10.1083/jcb.129.6.1543.

[2] A. Sorkin, M. McClure, F. Huang, R. Carter, Interaction of EGF receptor and Grb2 in living cells visualized by fluorescence resonance energy transfer (FRET) microscopy, Curr. Biol. 10 (2000) 1395–1398, https://doi.org/10.1016/S0960-9822(00)00785-5.

[3] Y. Xu, D.W. Piston, C.H. Johnson, A bioluminescence resonance energy transfer (BRET) system: application to interacting circadian clock proteins, Proc. Natl. Acad. Sci. U. S. A. 96 (1999) 151–156, https://doi.org/10.1073/pnas.96.1.151.

[4] G.A. Jones, D.S. Bradshaw, Resonance energy transfer: from fundamental theory to recent applications introduction and the early years of ret, Front. Phys. 1 (2019), https://doi.org/10.3389/fphy.2019.00100.

[5] A. De, R. Arora, A. Jasani, Engineering aspects of bioluminescence resonance energy transfer systems, in: Eng. Transl. Med., Springer-Verlag London Ltd, 2014, pp. 257–300, https://doi.org/10.1007/978-1-4471-4372-7_10.

[6] Y. Arai, T. Nagai, Real-time chemiluminescence imaging using nano-lantern probes, Curr. Protoc. Chem. Biol. 6 (2014) 221–236, https://doi.org/10.1002/9780470559277.ch140168.

[7] S. Dimri, S. Basu, A. De, Use of BRET to study protein-protein interactions in vitro and in vivo, in: Methods Mol. Biol., Humana Press Inc., 2016, pp. 57–78, https://doi.org/10.1007/978-1-4939-3724-0_5.

[8] L.A. Stoddart, E.K.M. Johnstone, A.J. Wheal, J. Goulding, M.B. Robers, T. Machleidt, K. V Wood, S.J. Hill, K.D.G. Pfleger, Application of BRET to monitor ligand binding to GPCRs, Nat. Methods 12 (2015) 661–663, https://doi.org/10.1038/nmeth.3398, 2015 127.

[9] K.A. Rumyantsev, K.K. Turoverov, V.V. Verkhusha, Near-infrared bioluminescent proteins for two-color multimodal imaging, Sci. Rep. 6 (2016) 36588, https://doi.org/10.1038/srep36588, 36588.

[10] A. De, A. Jasani, R. Arora, S.S. Gambhir, Evolution of BRET biosensors from live cell to tissue-scale in vivo imaging, Front. Endocrinol. 4 (2013) 131, https://doi.org/10.3389/fendo.2013.00131.

[11] M. Rathod, A. Mal, A. De, Reporter-based BRET sensors for measuring biological functions in vivo, in: Methods Mol. Biol., Humana Press Inc., 2018, pp. 51–74, https://doi.org/10.1007/978-1-4939-7860-1_5.

[12] A.A. Kotlobay, K.S. Sarkisyan, Y.A. Mokrushina, M. Marcet-Houben, E.O. Serebrovskaya, N.M. Markina, L. Gonzalez Somermeyer, A.Y. Gorokhovatsky, A. Vvedensky, K. V Purtov, V.N. Petushkov, N.S. Rodionova, T. V Chepurnyh, L.I. Fakhranurova, E.B. Guglya, R. Ziganshin, A.S. Tsarkova, Z.M. Kaskova, V. Shender, M. Abakumov, T.O. Abakumova, I.S. Povolotskaya, F.M. Eroshkin, A.G. Zaraisky, A.S. Mishin, S. V Dolgov, T.Y. Mitiouchkina, E.P. Kopantzev, H. E. Waldenmaier, A.G. Oliveira, Y. Oba, E. Barsova, E.A. Bogdanova, T. Gabaldón, C. V Stevani, S. Lukyanov, I. V Smirnov, J.I. Gitelson, F.A. Kondrashov, I. V Yampolsky, Genetically encodable bioluminescent system from fungi, Proc. Natl. Acad. Sci. U. S. A. 115 (2018) 12728–12732, https://doi.org/10.1073/pnas.1803615115.

[13] T. Mitiouchkina, A.S. Mishin, L.G. Somermeyer, N.M. Markina, T.V. Chepurnyh, E.B. Guglya, T.A. Karataeva, K.A. Palkina, E.S. Shakhova, L.I. Fakhranurova, S. V. Chekova, A.S. Tsarkova, Y.V. Golubev, V.V. Negrebetsky, S.A. Dolgushin, P.V. Shalaev, D. Shlykov, O.A. Melnik, V.O. Shipunova, S.M. Deyev, A.I. Bubyrev, A. S. Pushin, V.V. Choob, S.V. Dolgov, F.A. Kondrashov, I.V. Yampolsky, K.S. Sarkisyan, Plants with genetically encoded autoluminescence, Nat. Biotechnol. 38 (2020) 944–946, https://doi.org/10.1038/s41587-020-0500-9.

[14] A. Dragulescu-Andrasi, C.T. Chan, A. De, T.F. Massoud, S.S. Gambhir, Bioluminescence resonance energy transfer (BRET) imaging of protein-protein interactions within deep tissues of living subjects, Proc. Natl. Acad. Sci. U. S. A. 108 (2011) 12060–12065, https://doi.org/10.1073/pnas.1100923108.

[15] A. De, A.M. Loening, S.S. Gambhir, An improved bioluminescence resonance energy transfer strategy for imaging intracellular events in single cells and living subjects, Cancer Res. 67 (2007) 7175–7183, https://doi.org/10.1158/0008-5472.CAN-06-4623.

[16] J. Chen, X.F. Zheng, E.J. Brown, S.L. Schreiber, Identification of an 11-kDa FKBP12-rapamycin-binding domain within the 289-kDa FKBP12-rapamycin-associated protein and characterization of a critical serine residue, Proc. Natl. Acad. Sci. 92 (1995) 4947–4951, https://doi.org/10.1073/pnas.92.11.4947.

[17] N. Hay, N. Sonenberg, Upstream and downstream of mTOR, Genes Dev. 18 (2004) 1926–1945, https://doi.org/10.1101/gad.1212704.

[18] R.N. Saunders, M.S. Metcalfe, M.L. Nicholson, Rapamycin in transplantation: a review of the evidence, Kidney Int. 59 (2001) 3–16, https://doi.org/10.1046/J.1523-1755.2001.00460.X.

[19] T. Tian, X. Li, J. Zhang, mTOR signaling in cancer and mTOR inhibitors in solid tumor targeting therapy, Int. J. Mol. Sci. 20 (2019), https://doi.org/10.3390/IJMS20030755.

[20] J. Bové, M. Martínez-Vicente, M. Vila, Fighting neurodegeneration with rapamycin: mechanistic insights, Nat. Rev. Neurosci. 12 (2011) 437–452, https://doi.org/10.1038/NRN3068.

[21] A. De, S.S. Gambhir, Noninvasive imaging of protein-protein interactions from live cells and living subjects using bioluminescence resonance energy transfer, FASEB J. 19 (2005) 2017–2019, https://doi.org/10.1096/fj.05-4628fje.

[22] D. Raab, M. Graf, F. Notka, T. Schödl, R. Wagner, The GeneOptimizer Algorithm: using a sliding window approach to cope with the vast sequence space in multiparameter DNA sequence optimization, Syst. Synth. Biol. 4 (2010) 215–225, https://doi.org/10.1007/s11693-010-9062-3.

[23] S. Dimri, R. Arora, A. Jasani, A. De, Dynamic monitoring of STAT3 activation in live cells using a novel STAT3 Phospho-BRET sensor, Am. J. Nucl. Med. Mol. Imaging 9 (2019) 321–334. http://www.ncbi.nlm.nih.gov/pubmed/31976162.

[24] M. Renna, Commentary: overcoming mTOR resistance mutations with a new-generation mTOR inhibitor, Front. Pharmacol. 7 (2016) 272–276, https://doi.org/10.3389/fphar.2016.00431.

[25] J. Xie, X. Wang, C.G. Proud, mTOR inhibitors in cancer therapy, F1000Research 5 (2016) 2078, https://doi.org/10.12688/f1000research.9207.1.

[26] K.D.G. Pfleger, K.A. Eidne, Illuminating insights into protein-protein interactions using bioluminescence resonance energy transfer (BRET), Nat. Methods (2006), https://doi.org/10.1038/nmeth841.

[27] A. De, P. Ray, A.M. Loening, S.S. Gambhir, BRET3: a red-shifted bioluminescence resonance energy transfer (BRET)-based integrated platform for imaging protein-protein interactions from single live cells and living animals, FASEB J. 23 (2009) 2702–2709, https://doi.org/10.1096/fj.08-118919.

[28] E. Weber, C. Engler, R. Gruetzner, S. Werner, S. Marillonnet, A modular cloning system for standardized assembly of multigene constructs, PLoS One 6 (2011) e16765, https://doi.org/10.1371/journal.pone.0016765.

[29] B. Shi, M. Xue, Y. Wang, Y. Wang, D. Li, X. Zhao, X. Li, An improved method for increasing the efficiency of gene transfection and transduction, Int. J. Physiol. Pathophysiol. Pharmacol. 10 (2018) 95–104. http://www.ncbi.nlm.nih.gov/pubmed/29755642.